# Homology modeling of the structure of tobacco acetolactate synthase and examination of the model by site-directed mutagenesis*

Dung Tien Le[1], Moon-Young Yoon[2], Young Tae Kim[3], and Jung-Do Choi[1]*

[1] School of Life Sciences, Chungbuk National University, Cheongju 361-763, Korea
[2] Department of Chemistry, Hanyang University, Seoul 133-791, Korea
[3] Department of Microbiology, Pukyong National University, Busan 608-737, Korea

*To whom correspondence should be addressed. E-mail: jdchoi@cbucc.chungbuk.ac.kr

## Abstract

Acetolactate synthase (ALS, EC 4.1.3.18; also referred to as acetohydroxy acid synthase) catalyzes the first common step in the biosynthesis of valine, leucine, and isoleucine in microorganisms and plants. Recently X-ray structure of yeast ALS was available. Pair-wise alignment of yeast and tobacco ALS sequences revealed 63% sequence similarity. Using Deep View and automatic modeling on Swiss model server, we have generated reliable models of tobacco ALS based on yeast ALS template with a calculated pair-wise RMSD of 0.86 Angstrom. Functional roles of four residues located on the subunit interface (H142, E143, M350, and R376) were examined by site-directed mutagenesis. Seven mutants were generated and purified, of which three mutants (H142T, M350V, and R376F) were found to be inactivated under various assay conditions. The H142K mutant showed moderately altered kinetic properties. The E143A mutant increased 10-fold in $K_m$ value while other parameters remained unchanged. The M350C mutant was strongly resistant to three tested herbicides, while the R376K mutant can bind with herbicide carder at similar affinity to that of wild type enzyme, as determined by tryptophan quenching study. Except M350V mutant, all other mutants were able to bind with cofactor FAD. Taken together, it is likely that residues H142 and E143 are located at the active site, while residues M350 and R376 are possibly located at the overlapping region of active site and herbicide binding site of the enzyme. Our data also allows us to hypothesize that the interaction between side chains of residues M350 and R376 are probably essential for the correct conformation of the active site. It remains to be elucidated that, whether the herbicide, upon binding with enzyme, inactivates the enzyme by causing change in the active site allosterically, which is unfavorable for catalytic activity.

## Introduction

Acetolactate synthase (ALS, EC 4.1.3.18; also referred to as acetohydroxy acid synthase) catalyzes the first step in the biosynthesis of branched chain amino acids such as valine, leucine, and isoleucine in microorganisms and plants. ALS catalyzes the condensation of two molecules of pyruvate to give rise to 2-acetolactate in the first step of valine and leucine biosynthetic pathway, and in parallel, it also catalyzes the condensation of pyruvate and 2-ketobutyrate to yield 2-aceto-2-hydroxybutyrate in the second step of isoleucine biosynthesis [1].

ALS requires thiamine pyrophosphate (TPP), flavin adenine dinucleotide (FAD), and divalent metal ion, Mg2+ or Mn2+ as cofactors for its catalytic function. Much attention has been paid to ALS since it was demonstrated to be the target of several classes of herbicides, including the sulfonylureas [2, 3], the imidazolinones [4], and the triazolopyrimidines [5, 6].

Three bacterial ALS isozymes have been purified and studied extensively in terms of their genetic regulation, kinetic properties, feedback

* This work was supported by Korea Research Foundation Grant, *KRF-2002-070-C0064*

regulation, and sensitivity to herbicidal inhibitors [7-10]. Each of the isozymes is a tetramer of two large catalytic subunits (59-60 kDa) and two small regulatory subunits (9-17 kDa) [1]. In contrast to the bacterial enzyme, the structure and biochemical properties of ALS from eukaryotes have not been well characterized since purification of eukaryotic ALS is severely hampered by its extreme instability and very low abundance.

Recently, our site-directed mutagenesis studies showed that K219 [11], W490 [12], C411 [13], H487 [14], and M512 [15] residues are essential for catalytic function of tobacco ALS, and that K255 [11], W573 [12], A121 [16], S652 [16], and M569 [15] are possibly located at herbicide-binding site. More recently, preliminary X-ray diffraction analysis of the catalytic subunit of yeast ALS was reported [17, 18].

Before the X-ray structure of yeast ALS was reported, several efforts had been made to understand the structure-function relationship of ALS by homology modeling based on X-ray structure of other TPP-dependent enzymes [19, 20]. Ibdah *et al.* [19] reported the homology modeling and examination of the active site of bacterial ALS, while Ott *et al.* [20] proposed an approach employing homology modeling and site-directed mutagenesis to design herbicide resistant ALS.

Alignment of ALS sequences from tobacco and yeast revealed 41% and 63% sequence identity and similarity, respectively. Thus, in this study, we carried out homology modeling for catalytic subunits of tobacco ALS based on yeast ALS X-ray structure (1JSC.pdb and 1N0H.pdb) using Deep View and remotely automatic modeling at Swiss Model server. The roles of fours residues locate at the subunit interface were studied using site-directed mutagenesis.

## Materials and methods

### Materials

Bacto-tryptone, yeast extract, and Bacto-agar were purchased from Difco Laboratories (Detroit, USA). Restriction enzymes were purchased from Takara Shuzo Co. (Shiga, Japan) and Boehringer-Mannheim (Mannheim, Germany). GSH, TPP, FAD, α-naphthol, and creatine were obtained from Sigma Chemical Co. (St. Louis, USA). Thrombin protease and epoxy-activated Sepharose 6B were obtained from Pharmacia Biotech (Uppsala, Sweden). *E. coli* XL1-blue cells containing expression vector pGEX-ALS were provided by Dr. Soo-Ik Chang (Chungbuk National University, Cheongju, Korea). Oligonucleotides were obtained from Jenotech (Taejon, Korea). Londax (a sulfonylurea herbicide) and Cadre (an imidazolinone herbicide) were kindly provided by Dr. Dae-Whang Kim (Korea Research Institute of Chemical Technology, Taejon, Korea). TP, a triazolopyrimidine derivative, was obtained from Dr. Sung-Keon Namgoong (Seoul Women's University, Seoul, Korea).

### Homology modeling of tobacco catalytic subunit

The sequences of ALS from tobacco and yeast were aligned on BioEdit program [21]. 92 N-terminal amino acid residues of the tobacco ALS corresponding to the transit peptide was removed, the resultant sequence were fitted on the X-ray structure yeast ALS using Deep View. The resulting alignment was examined manually and then submitted for automatic modeling at Swiss model server [22, 23]. Using this approach a model of single catalytic subunit of tobacco ALS was successfully obtained. The modeling job was then carried out using oligomer modeling approach as described at Swiss model website. Two models of tobacco ALS homodimer were obtained based on two different X-ray coordinates (with and without the present of a herbicide, 1N0H.pdb, 1JSC.pdb). A single round of energy minimization was done with the GROMOS96 implemented on Deep View.

### Multiple sequence alignment of ALS sequences

We aligned 39 ALS sequences of plants, bacteria and alga using ClustalW program [24], which was integrated in BIOEDIT Software [21] provided by North Carolina State University. Data set consists of ALS sequences from following species: *A. powellii, A. retroflexus, A. spp., A. thaliana, B. napus., B. napus, B. napus, B. scoparia, C. caldarium, Guillardia theta, N. tabacum, P. purpurea, R. raphanistrum, S. platensis, S. ptychanthum, Volvox carteri, B. subtilis, A. pisum, S. graminum, S. chinensis, C. acetobutylicum, C. glutamicum, E. coli, H. influenzae, K. pneumoniae, L. lactis sub. Lactis, M. grisea, M. jannaschii, M. avium, M. leprae, M. tuberculosis, R. terrigena, S. cerevisiae, S. typhimurium, S. pombe.*

**Site-directed mutagenesis**

Site-directed mutagenesis of tobacco ALS was performed directly on the plasmid derived from pGEX-2T containing tobacco ALS cDNA, using the PCR megaprimer method [25]. All manipulations of the DNA were carried out using the technique reported previously [26]. The PCR was also performed as described by Saiki *et al.* [27]. The first PCR was carried out with oligonucleotide primer NKB2 and each mutagenic fragment as internal primers with the underlined bases changed:
NKB2, 5'-CCCG**GGATCC**TCAAAGTCAATA-3'
H142K, 5'- CTACCACGTAAGGAGCAG G -3'
H142T, 5'- CTACCACGTACCGAGCAG G -3'
E143A, 5'- CCACGTCACGCTCAGGGT -3'
M350C, 5'- GTTGGGTTGTCATGGTACTGTTTA-3'
M350V, 5'- GTTGGGTGTGCATGGTACTGTTTA-3'
R376F, 5'- GAGGTTTGATGATTTCGTTACTGG -3'
R376K, 5'-GAGGTTTGATGATAAAGTTACTGG -3'
The bold bases in the NKB2 primer are *BamH*I restriction sites. Each reaction mixture contained 50 ng of template DNA, 25 pmol of mutagenic primer and universal primer NKB2, 200 μM dNTPs, and Taq polymerase in 50 mM KCl, 10 mM Tris (pH 7.5) and 1.5 mM $MgCl_2$ in 100 μl. The resulting DNA was subjected to a second PCR with the universal primer NKB1 5'-CATCTCC**GGATCC**ATGTCCACTACCCA A-3'. The PCR products were double digested with *Nco*I and *Bgl*II, and cloned into the expression vector, which was prepared from the *Nco*I/*Bgl*II-excised pGEX-wALS. The resulting pGEX-mALS was used to transform the *E. coli* strain XL1-Blue cells using standard $CaCl_2$ transformation instructions [30]. Each transformant was identified by digestion of plasmid with *BamH*I, transformants give correct restriction map were sequenced to ensure the correct base mutation in the mutant ALS gene. *E. coli* BL21-DE3 cells carrying correct mutant ALS plasmid was cultured to obtain the mutant protein.

**DNA sequence analysis**

DNA sequencing was carried out by the dideoxy chain-termination procedure [28] on an ABI Prism 3700 automatic DNA sequencer at Macrogen, Inc. (Seoul, Korea). Each mutant ALS was sequenced and identified.

**Expression and purification of tobacco wALS and mALS**

Bacterial strains of *E. coli* BL21-DE3 cells containing the expression vector pGEX-ALS were grown at 37°C in Luria-Bertani (LB) medium containing 50 μg/ml ampicilin to an $OD_{600}$ of 0.7-0.8. Expression of the pGEX-ALS gene was induced by adding 0.1-0.3 mM isopropyl-D-thiogalactoside (IPTG). Cells were grown for an additional 3 hours at 30°C, and harvested by centrifugation at 5000 g for 30 min. Purification of wALS and mALS was carried as described previously [12, 15, 16]. The cell pellets were suspended with the standard buffer (50 mM Tris-HCl, pH 7.5, 1 mM pyruvate, 10% (v/v) ethylene glycol, 10 mM $MgCl_2$) containing protease inhibitors (2 μg/ml leupeptin, 4 μg/ml aprotinin, 2 μg/ml pepstatin A). The cell suspension was then lysed by sonication at 4°C. The homogenate was centrifuged at 20,000 g for 20 min and the supernatant was re-centrifuged. The supernatant was applied to the GSH-coupled Sepharose 6B column and unbound proteins were removed by washing with the standard buffer. Then, the GST-ALS fusion protein was recovered from the column with an elution buffer (50 mM Tris-HCl, pH 7.5, 15 mM GSH, and 10% (v/v) ethylene glycol). To obtain the cleaved ALS, the purified GST-ALS was incubated overnight at 4°C with thrombin (10U/mg protein). The ALS was purified by an additional step of GSH-affinity chromatography. The isolated protein was identified by SDS-PAGE analysis [29], and the protein concentration was determined by the method of Bradford [30].

**Molecular mass determination by size-exclusion chromatography**

ALS was first purified by affinity chromatography to homogeneity. The sample was then passed through a Sephadex G-200, which was pre-equilibrated with sample buffer, to remove the aggregation portion. The active peak was pooled, concentrated and used as loading sample for FPLC.
400ul of wALS was loaded onto a Superdex 200, HiLoad 16/60 column (Amersharm Biosciences) connected to an ÄKTApurifier 10 (Amersham Biosciences). The whole system was monitored by a computer running UNICORN software. The system was equilibrated with sample buffer. Flow rate was set at 0.8 ml/min; detection wavelengths were set at 280 nm and 260 nm. High molecular weight gel filtration calibration kit (Amersham Biosciences) was used as standard.

**Enzyme assay**

Enzyme activities of the purified wALS and

mALS were measured according to the method of Westerfeld [31] with a modification as reported previously [32]. The reaction mixture contained a 50 mM potassium phosphate buffer (pH 7.5), 1 mM TPP, 10 mM $MgCl_2$, 20 μM FAD, 100 mM pyruvate, and the enzyme in the absence or presence of various concentrations of inhibitors. Assay was terminated by adding 6 N $H_2SO_4$, and then the reaction product acetolactate was allowed to decarboxylate. The acetoin formed by acidification was colorized with 0.5% creatine and 5% α-naphthol. The absorbance of the reaction mixture was determined at 525 nm.

### Spectroscopic measurement

Absorption spectra were recorded on Beckman DU-600 Spectrophotometer. The protein solution was dispensed in 1 ml black-walled quartz cuvettes, and the spectrum of each sample was scanned over the range of 250-550 nm. Fluorescence emission spectra were recorded with a Perkin Elmer Luminescence Spectrophotometer LS50B. The fluorescence spectra of FAD bound to wALS and mALS were scanned over the range of 450-650 nm by exciting at 450 nm. Tryptophan fluorescence spectra were recorded over the range of 300-400 nm by exciting at 295 nm. The CD spectra were recorded over the range of 200-250 nm on a Jasco J-710 Spectropolarimeter set at 20-50 mdeg sensitivity, 1 mm resolution, 3 units accumulation, 5 seconds response, and at a scanning speed of 200 nm/min. A protein solution of 0.2-0.6 mg/ml was assayed in a 1 mm-path length cylindrical quartz cell.

## Result

### Homology modeling of tobacco ALS

The pair-wise alignment of tobacco and yeast ALS sequences was carried out as described in figure legend and Materials and Methods. Alignment of partial sequences (after removal of transit peptide) of the two species revealed 41% and 63% sequence identity and similarity, respectively (Figure 1).

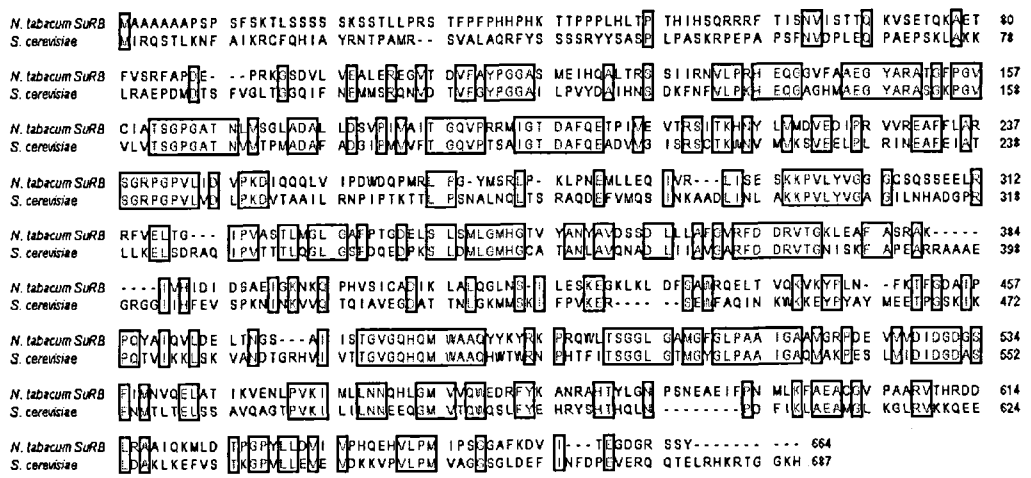

*Figure 1:* Pair-wise alignment of complete sequences of tobacco and yeast ALS. Alignment was done using BIOEDIT software with matrix PAM250, gap initial penalty = 8, gap extension penalty = 2. Identical residues are boxed and in red, similar residues are in blue, other residues are in black.

**Table 1: Root mean square Z-scores**

| RMS Z-scores | |
|---|---|
| Bond lengths | 1.837 |
| Bond angles | 1.141 |
| Omega angle restrains | 1.087 |
| Side chain planarity | 1.627 |
| Improper dihedral distribution | 1.140 |
| Inside/Outside distribution | 1.109 |

The partial sequence of tobacco ALS was fitted on the X-ray structure of yeast ALS. The alignment was examined manually. The optimized project was submitted for automatic modeling at Swiss model server (Function integrated within Deep View). Two models based on two separate X-ray structures of yeast ALS were obtained. The RMS Z-scores returned by WhatCheck [33, 34] (Table 1) and the

Ramachandran plot [35] (Figure 2) showed that the models obtained were highly reliable. Figure 3 shows the superimposition of backbones of tobacco ALS model on yeast ALS template.

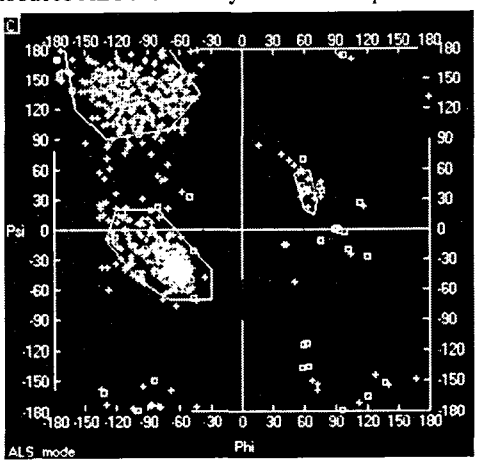


*Figure 2:* Ramachandran plot of the main-chain dihedral angles (Phi, Psi) for Tobacco ALS dimer model based on 1JSC.pdb. Rectangular sign represents glycine residues, plus sign represents other residues.

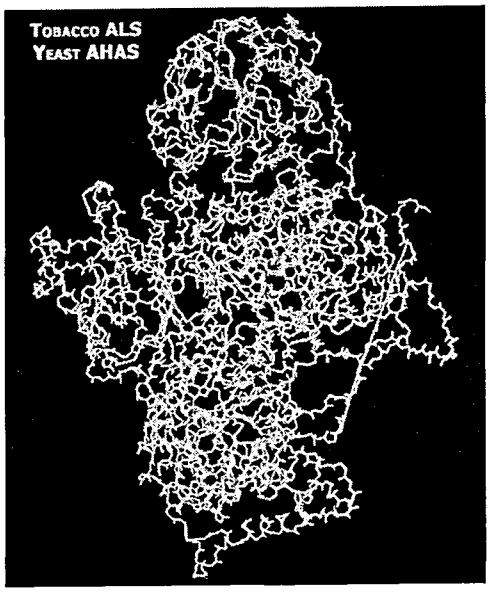


*Figure 3*: Superimposition of backbones of Tobacco ALS model on Yeast ALS X-ray structure (1JSC.pdb). Pair-wise RMSD = 0.86 Angstrom, The long loop corresponds to the missing residues on the template.

**Identification of subunit interface residues**

To identify whether tobacco ALS does present as oligomer form practically, we employed native-PAGE. The native-PAGE data showed a single band moving slower than the standard band of 250kDa (data not shown). It seems that the enzyme does not present as monomer form, since it had been reported to be a 65 kDa polypeptide [11-15]. The molecular mass of the enzyme complex was determined promptly by size-exclusion chromatography employing a AKTApurifier 10 system to be 365.3 kDa. It is likely that the enzyme complex presents in hexamer form.

On the model, we have identified more than a hundred residues on each subunit located within 6 Angstrom from the interface of other subunit, of which, the functional roles of 4 well-conserved residues (H142, E143, R376, M350) were examined by site-directed mutagenesis.

**Kinetic properties of wild type and mutant enzymes**

To examine the functions of selected residues, seven mutants were successfully generated and purified to be a single band on SDS-PAGE similar to that of wild type enzyme (data not shown). The mutant and wild-type enzymes were characterized in term of kinetic parameters, including $V_{max}$, $K_m$, $K_c$ for FAD, TPP and $K_i^{app}$ of three herbicides, Londax, Cadre, and TP4. The values of $V_{max}$, and $K_m$ for the substrate were determined by fitting the data to Equation (1), while the values of activation constant ($K_c$) were obtained by fitting the data to equation (2), by the non-linear least-squares and Simplex methods for error minimization [36].

$$v = V_{max}/(1+K_m/[S]) \qquad (1)$$

$$v = V_0 + V_{max}/(1+K_c/[C]) \qquad (2)$$

In these equations, v is the reaction velocity, $V_{max}$ is the maximum velocity, $V_0$ is the activity without adding cofactors, $K_m$ is Michaelis Menten constant, $K_c$ is activation constant, [S] is substrate concentration, and [C] is added cofactor concentration. Table 2 shows the values of $V_{max}$, $K_m$, $K_c$ for the cofactors, and $K_i^{app}$ for the inhibition by herbicides. Three mutants H142T, M350V, and R376F were inactivated under various assay conditions. The $K_m$ values for pyruvate of H142K, E143A, M350C and R376K were 94.9, 53.83, 56.69 and 16.44 mM, respectively.

*Table 2:* **Kinetic properties of wild type and mutant enzymes**

| | Km (mM) | Specific activity | $K_{FAD}$ (μM) | $K_{TPP}$ (mM) | $IC_{50}$ Cardre (μM) | $IC_{50}$ Londax (nM) | $IC_{50}$ TP4 (μM) |
|---|---|---|---|---|---|---|---|
| wALS | 4.83 | 0.45 | 4.56 | 0.29 | 6.59 | 8.80 | 18.87 |
| H142K | 94.9 | 0.14 | - | - | 123.22 | 195.46 | 34.87 |
| H142T | | | | | *No activity* | | |
| E143A | 53.83 | 0.66 | 7.06 | 0.16 | 2.67 | 8.32 | 12.69 |
| M350C | 56.69 | 0.031 | 51.54 | 0.83 | ND | 907.4 | ND |
| M350V | | | | | *No activity* | | |
| R376F | | | | | *No activity* | | |
| R376K | 16.44 | 0.002 | - | 0.25 | 22.50 | 75.87 | 51.28 |

*TP4, a newly synthesized Triazolopyrimidine; ND, not detectable within the range of 0-128 μM*

**Spectral properties of wild type and mutant enzyme**

Though expressed as intact protein (data not shown), H142T, M350V, and R376F mutants were inactive under various assay conditions. To understand the mechanism of inactivation, we measured the absorption and fluorescence spectra of wild-type and mutant enzymes. Data on figure 4 (and data not shown) showed that, among the inactive mutants, only M350V mutant was not able to bind with FAD, while other mutants can bind at a lower affinity than that of wild type enzyme (Figure 4, inset).

To determine whether there is any change in secondary structure of the mutant enzymes, we measured CD spectra of wild type and mutant ALSs. Result on figure 5 (and data not shown) showed that the CD spectra of all mutants almost completely overlapped with that of wild type enzyme. This data indicates that all substitutions in this study did not perturb the secondary structure of the enzyme.

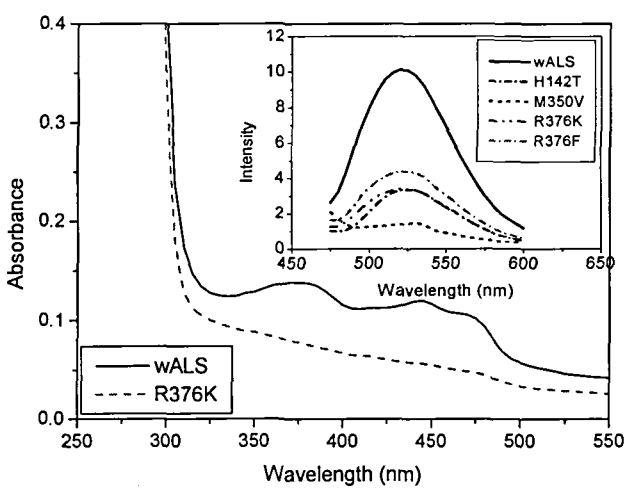


*Figure 4:* Absorption and fluorescence spectra of wild type and mutant enzymes. Concentration of each enzyme was at 0.9 mg protein/mL in 50 mM Tris-Cl buffer (pH 7.5).

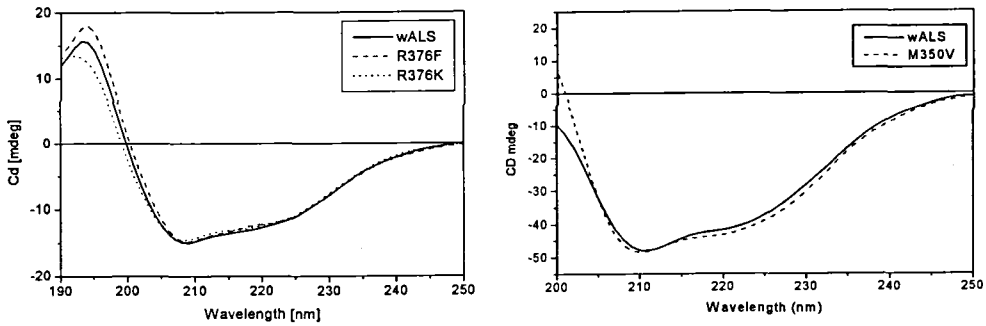


*Figure 5:* CD spectra of wild type and mutant enzymes. Each protein was present at a concentration ranging from 0.20 to 0.60 mg/mL in 10 mM potassium phosphate buffer (pH 7.5).

**Interaction with herbicides**

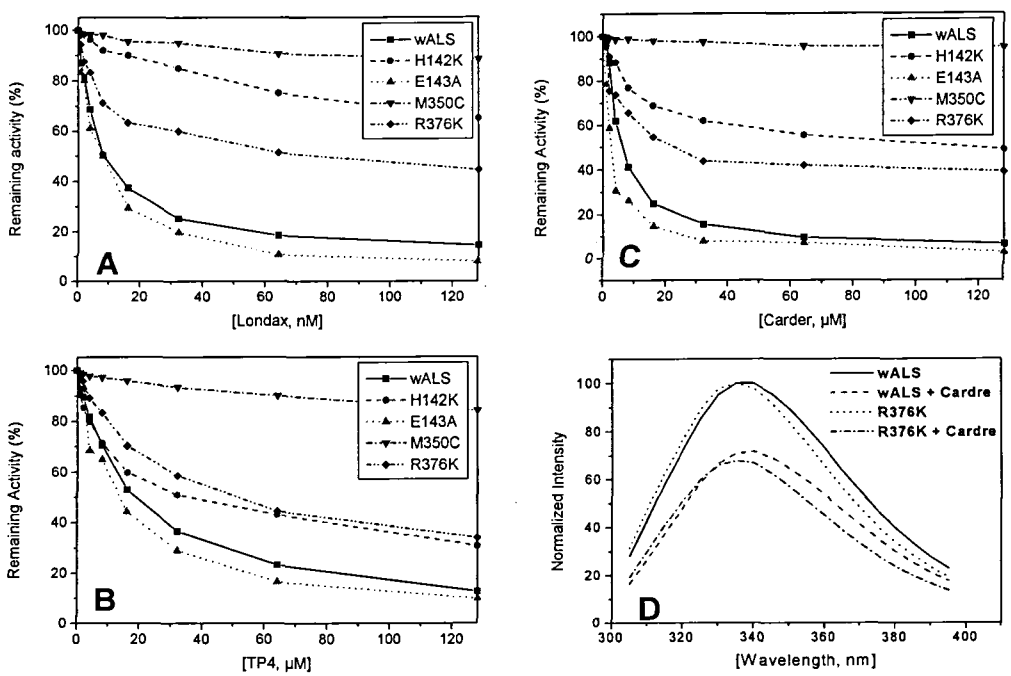


*Figure 6:* Effects of three classes of herbicides (A - the sulfonylurea Londax, B - the imidazolinone Cardre, and D - the triazolopyrimidine TP4) on wild-type and mutant enzymes. D- Tryptophan quenching study of wALS and R376K mutant. Tryptophan fluorescence was measured before and after 64 µM carder was added to the enzyme solutions and allowed incubation for 10 minutes at room temperature.

The herbicide sensitivity of four active mutants (H142K, E143A, M350C and R376K) were compared to that of wild type enzyme for three classes of herbicides, Londax (a sulfonylurea), Cadre (an imidazolinone), and TP4 (a

triazolopyrimidine). The $K_i^{app}$ were determined by fitting the data to Equation (3).

$$v_i = v_0/(1+[I]/K_i^{app}) \quad (3)$$

In this equation, $v_i$ and $v_0$ represent the rate in the presence or absence of the inhibitor, respectively, and [I] is the concentration of the inhibitor. The $K_i^{app}$ is the apparent $K_i$, that is the concentration of the inhibitor giving 50% inhibition under a standard assay condition, which is also known as $IC_{50}$. The M350C mutant was highly resistant to three tested herbicides, londax, carder, and TP4. The H142K mutant was strongly resistant to londax but moderately resistant to carder and TP4. The R376K mutant was slightly resistant to three tested herbicides. The E143A mutant did not show any resistance to the three tested herbicides (Figure 6). Since the specific activity of R376K mutant was quite low, the activity inhibition assay may not give an accurate result. Thus, we carried out tryptophan quenching study on wild type enzyme and R376K mutant using herbicide carder as the quencher. Data on figure 7-D showed that, the binding of carder to wALS was associated with tryptophan quenching and the same level of quenching was detected with R376K mutant.

## Discussion

### The role of residues H142 and E143

On the model, residue H142 was found to make a hydrogen bond to side chain of Q144 of the other subunit (Figure 7). The side chain of E143 was found to make an H-bond to TPP molecule. In addition, these two residues are identical in 39 ALS sequences.

The substitution of residue H142 by threonine inactivated the enzyme. This result indicated that residue H142 is essential for the catalytic activity of the enzyme. It is interesting that, the substitution of residue E143 by amino acid alanine resulted in only a 10-fold increase in $K_m$ value, while other parameters remained unaffected. This evidence strongly supports the idea that the negatively charged side chain of E143 probably involve in binding with pyruvate. Since it has been identified on the model to be hydrogen-bonded to TPP, it is likely that the side chain of residue E143 involve in binding with pyruvate indirectly via TPP. The residue equivalent to tobacco E143 in ALSs of other species had been reported to play certain roles in catalysis [1]. Though located next to E143, where the mutation did not affect herbicide binding, the H142K mutant showed changes in both catalytic property as well as herbicide sensitivity. [This is probably due to loosening of the dimer complex].

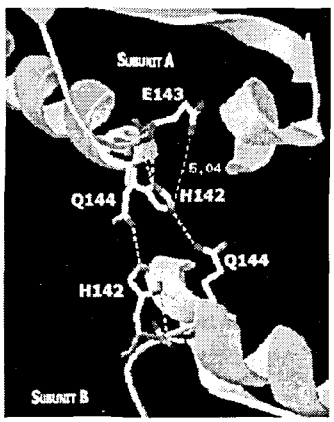


*Figure 7:* Structure surrounding residues H142 and E143 of tobacco ALS. Model obtained based on X-ray structure of yeast AHAS (1JSC.pdb).

### The roles of residues M350 and R376

On the two models we generated, residues M350 and R376 are found to be close together and close to a known herbicide related residue (H351) [14]. On the model generated based on 1JSC.pdb (without herbicide), side chain of R376 was hydrogen-bonded to side chains of M350 and H351 (Figure 8, left), while on the model generated based on 1N0H.pdb (with herbicide) the side chain of R376 was found to interact with herbicide molecule (Figure 8, right).

Using the mutation function of Deep View, we found that, on the model generated based on 1JSC.pdb the hydrogen bond between side chains of residues M350 and R376 was broken when either the residue M350 was mutated to valine or the residue R376 was mutated to lysine or phenylalanine. Coincidentally, the mutants of M350V, R376F were found to be inactive experimentally without changing in secondary structure.

The "conservative substitution" of R376 by lysine resulted in a mutant whose activity was 225-fold lower than that of wild type enzyme. The tryptophan quenching study showed that the R376K mutant can bind to herbicide carder, which produced a quenching effect similar to that when carder is bound to wild type enzyme. The substitution of M350 by cysteine did not break the hydrogen bond between itself and R376, the

M350C mutant was practically active and strongly resistant to three tested herbicides. Taken together, it is likely that the interaction between side chains of M350 and R376 is essential for correct formation of the active site.

On the model of enzyme-herbicide complex, the hydrogen bond between the side chains of residues R376 and M350 was not presented, instead, the side chain of R376 was hydrogen bonded to the herbicide molecule. Assuming that the complex is enzymatically inactive (inhibition), we could hypothesize that, in this case, the herbicide, upon binding to the enzyme, inhibits the enzyme activity by causing a change in structure of the active site, which is unfavorable for catalytic function.

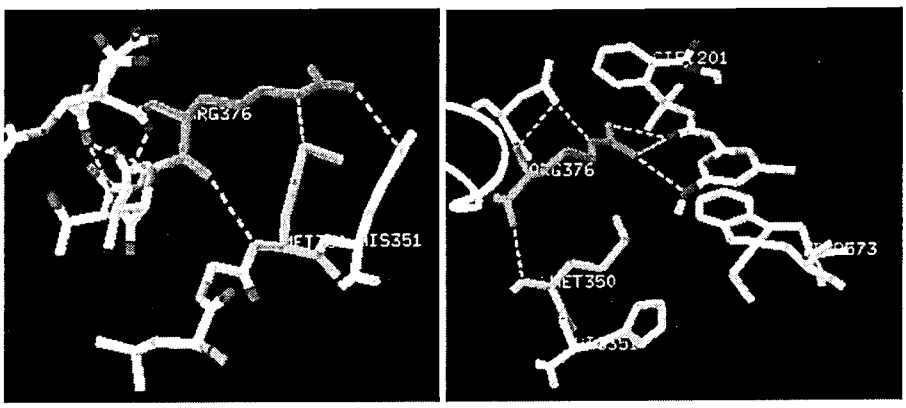


***Figure 8:*** Structure surrounding residues M350 and R376. Left – model generated based on 1JSC.pdb; Right – model generated based on 1N0H.pdb (enzyme-herbicide complex)

## Conclusion

Two reliable models of tobacco ALS were successfully generated using Deep View and remotely automatic modeling on Swiss model server.

Conserved subunit interface residues were identified. Functional roles of 4 residues, H142, E143, M350 and R376 were examined experimentally by site directed mutagenesis.

It is likely that the residues H142 and E143 are located at the active site, furthermore, residue E143 probably involves in binding with pyruvate. The residues M350 and R376 are possibly located at the overlapping region between active site and a common herbicide binding site.

## References


[1] Duggleby, R. G., and Pang, S. S. (2000) Acetohydroxyacid Synthase. *J. Biochem. Mol. Biol.* **33**, 1-36.

[2] LaRossa, R. A., and Schloss, J. V. (1984) The sulfonylurea herbicide Sulfometuron is an extremely potent and selective inhibitor of acetolactate synthase in *Salmonella typhimurium*. *J. Biol. Chem.* **259**, 8753-8757.

[3] Ray, J. B. (1984) Site of action of chlorosulfuron: Inhibition of valine and isoleucine biosynthesis of plants. *Plant Physiol.* **75**, 827-831.

[4] Shaner, D. L., Anderson, P. C., and Stidham, M. A. (1984) Imidazolinones: potent inhibitors of acetohydroxy acid synthase. *Plant Physiol.* **76**, 545-546.

[5] Gerwick, B. C., Subramanian, M. V., Loney-Gallant, V., and Chander, D. P. (1990) Mechanism of action of the 1, 2, 4-triazolo [1, 5, a-] pyrimidine. *Pestic. Sci.* **29**, 357-364.

[6] Namgoong, S. K., Lee, H. J., Kim, Y. S., Shin, J.-H., Che, J.-K., Jang, D. Y., Kim, G. S., Yoo, J. W., Kang. M.-K., Kil, M.-W., Choi, J.-D., and Chang, S.-I. (1999) Synthesis of the quinoline-linked triazolopyrimidine analogues and their interactions with the recombinant tobacco acetolactate synthase. *Biochem. Biophys, Res. Commun.* **258**, 797-801.

[7] Schloss, J. V., Dyk, K. E. V., Vasta, J. F., and Kutny, B. M. (1985) Purification and properties of *Salmonella typhimurium* acetolactate synthase isozyme II from

*Escherichia coli* HB101/pDU9. *Biochemistry* **24**, 4952-4959.

[8] Barak, Z., Chipman, D. M., and Gollop, N. (1989) Physiological implications of the specificity of acetohydroxy acid synthase isozymes. *J. Bacteriol.* **169**, 3750-3756.

[9] Eoyang, L., and Silverman, P. M. (1988) Purification and assays of acetolactate synthase I from *Escherichia coli* K12. *Methods Enzymol.* **166**, 435-445.

[10] Hill, C. M., and Duggleby, R. G. (1998) Mutagenesis of *Escherichia coli* acetohydroxy acid synthase II and characterization of three herbicide-resistant forms. *Biochem. J.* **335**, 653-661.

[11] Yoon T.-Y., Chung S.-M., Chang S.-I., Yoon M.-Y., Hahn T.-R., and Choi J.-D. (2002) Roles of lysine 219 and 255 residues in tobacco acetolactate synthase. *Biochem. Biophys. Res. Comm.* 293, 433-439

[12] Chong, C.-K., Shin, H.-J., Chang, S.-I., and Choi, J.-D. (1999) Role of tryptophanyl residues in tobacco acetolactate synthase. *Biochem. Biophys. Res. Commun.* **259**, 136-140.

[13] Shin, H.-J., Chong, C.-K., Chang, S.-I., and Choi, J.-D. (2000) Structural and functional role of cysteinyl residues in tobacco acetolactate synthase. *Biochem. Biophys. Res. Commun.* **271**, 801-806.

[14] Oh, K.-J., Park, E.-J., Yoon, M.-Y., Han, J.-R., and Choi, J.-D. (2001) Roles of histidine residues in tobacco acetolactate synthase. *Biochem. Biophys. Res. Commun.* **282**, 1237-1243.

[15] Le, D. T., Yoon M.-Y., Kim, Y. T., Choi, J.-D (2003). Roles of conserved methionine residues in tobacco acetolactate synthase. *Biochem. Biophys. Res. Commun.* **306** (4): 1075-1082.

[16] Chong, C.-K., and Choi, J.-D. (2000) Amino acid residues conferring herbicide tolerance in tobacco acetolactate synthase. *Biochem. Biophys. Res. Commun.* **279**, 462-467.

[17] Pang, S. S., Guddat, L. W., and Duggleby, R. G. (2001) Crystallization of the catalytic subunit of *Sacharomyces cerevisiae* acetohydroxyacid synthase. *Acta Cryst.* **D57**, 1321-1323.

[18] Pang, S. S., Guddat, L. W., and Duggleby, R. G. (2003) Molecular basis of Sulfonylureas herbicide inhibition of acetohydroxyacid synthase. *J. Biol. Chem.* **278**, 7639-7644.

[19] Ibdah, M., Bar-Ilan, A., Livnah, O., Schloss, J. V., Barak, Z., and Chipman, D. M. (1996) Homology modeling of the structure of bacterial acetohydroxy acid synthase and examination of the active site by site-directed mutagenesis. *Biochem.* **35**, 16282-16291.

[20] Ott, K.-H., Kwagh, J.-G., Stockton, G. W., Sidrov, V., and Kekefuva, G. (1996) Rational molecular design and genetic engineering of herbicide resistance crops by structure modeling and site-directed mutagenesis of acetohydroxyacid synthase. *J. Mol. Biol.* **263**, 359-367.

[21] Hall, T.A. (1999) BioEdit: a user-friendly biological sequence alignment editor and analysis program for Windows 95/98/NT. *Nucl. Acids. Symp. Ser.* **41**:95-98.

[22] Schwede T, Kopp J, Guex N, and Peitsch MC (2003) SWISS-MODEL: an automated protein homology-modeling server. *Nucl. Acids Res.* **31**: 3381-3385.

[23] Guex, N. and Peitsch, M. C. (1997) SWISS-MODEL and the Swiss-PdbViewer: An environment for comparative protein modelling. *Electrophoresis* **18**:2714-2723.

[24] Thompson, J.D., Higgins, D.G., and Gibson, T.J. (1994) CLUSTALW: improving the sensitivity of progressive multiple sequence alignment through sequence weighting, positions-specific gap penalties and weight matrix choice. *Nucl. Acids Res.* **22**, 4673-4680.

[25] Sarkar, G., and Sommer, S. S. (1990) "Megaprimer" method of site-directed mutagenesis. *Biotechniques* **2**, 404-407.

[26] Sambrook, J., Fritsch, E. F., and Maniatis, T. (1989) Molecular Cloning: A Laboratory Manual, 2nd ed., *Cold Spring Harbor Laboratory Press*, Cold Spring Harbor, New York, USA.

[27] Saiki, R. K., Gelfand, D. H., Stoffel, S., Scharf, S. J., Higuchi, R., Horn, G. T., Mullis, K. B., and Erlich, H. A. (1988) Primer-directed enzymatic amplification of DNA with a thermostable DNA polymerase. *Science* **239**, 487-491.

[28] Sanger, F., Nicklen, S., and Coulson, A. R. (1977) DNA sequencing with chain-terminating inhibitors. *Proc. Natl. Acad. Sci. USA* **74**, 5463-5467.

[29] Laemmli, U. K. (1970) Cleavage of structural proteins during the assembly of the head of bacteriophage T4. *Nature* **227**, 680-685.

[30] Bradford, M. M. (1976) A rapid and sensitive method for the quantification of

microgram quantities of protein utilizing the principle of protein-dye binding. *Anal. Biochem.* **72**, 248-254.

[31] Westerfeld, W. W. (1945) A colorimetric determination of blood acetoin. *J. Biol. Chem.* **161**, 495-502.

[32] Chong, C.-K., Chang, S.-I., and Choi, J.-D. (1997) Functional amino acid residues of recombinant tobacco acetolactate synthase. *J. Biochem. Mol. Biol.* **30**, 274-279.

[33] Hooft, R.W.W., Vriend, G., Sander, C. and Abola, E.E. (1996) Errors in protein structures. *Nature* **381**, 272.

[34] Vriend, G. (1990) WHAT IF: a molecular modeling and drug design program. *J. Mol. Graph.* **8**, 52-56.

[35] Ramachandran, G.N., Ramakrishnan, C. and Sasisekharan, V. (1963) Stereochemistry of Polypeptide Chain Conformations *J. Mol. Biol.* **7**, 95-99.

[36] Nelder, J. A. and Mead, R. (1965) A simplex method for function minimization. *Comput. J.* **7**, 308-313.